Stabilization of Neoclassical Tearing Modes in Tokamak Fusion Plasmas via Extremum Seeking

William Wehner and Eugenio Schuster

***Abstract*— The neoclassical tearing mode (NTM) instability produces magnetic islands in tokamak plasmas that can degrade confinement and lead to plasma disruptions. NTMs are driven by a lack of bootstrap current inside the magnetic island where the pressure profile is flattened. Suppression of these islands is necessary for sustained energy confinement and efficient operation in tokamak magnetic-fusion reactors. Compensating for the lack of bootstrap current by an Electron Cyclotron Current Drive (ECCD) has been proved experimentally as an effective method to stabilize NTMs. The effectiveness of this method is limited in practice by the uncertainties in the width of the island, the relative position between the island and the EC beam, and the EC power threshold for NTM stabilization. Heuristic search and suppress algorithms have been proposed and shown effective to improve the alignment of the EC beam with the island by just using an estimate of the island width. Making use of this estimate, a real-time, non-model-based, extremum-seeking optimization algorithm is proposed in this work for EC beam steering and modulation in order to minimize the island-beam misalignment and the time (control energy) required for NTM stabilization. The efficiency of the proposed method is compared with traditional search and suppress algorithms.**

I. Introduction

Increasing the pressure in a resistive plasma can make the nested magnetic surface topology (Fig. 1-a) predicted by perfectly conducting ideal magnetohydrodynamic (MHD) plasmas [1] unstable, producing tearing and reconnection of the flux surfaces (hence the name tearing mode), and resulting in a structure called magnetic island (Fig. 1-b) [2]. The neoclassical tearing mode (NTM) is linearly stable but nonlinearly unstable. This implies on the one hand that a "seed" magnetic island induced by other instabilities [3], such as sawtooth precursors or edge localized modes (ELMs), must grow above a threshold island width for the island to grow large to a saturated size and persist stably in the plasma. On the other hand, if the island width can be decreased below this threshold, the mode will decay and vanish. The NTM develops on flux surfaces with rational safety factor $q = m/n$, m being the poloidal mode number and n the toroidal number.

The onset of NTM's have been shown to limit the achievable plasma performance in tokamaks by enhancing heat transport, reducing energy confinement time, and reducing the achievable β (=plasma pressure/magnetic pressure). If the magnetic islands driven by NTMs were allowed to grow to their maximum saturated widths in ITER, recent simulations [4] indicate that those magnetic islands would cover about a third of the plasma and would reduce the fusion power production by about a factor of four. Therefore, stabilization of NTMs, which are expected to occur in reactor-grade tokamaks such as ITER, is one of the most critical issues in tokamak reactors since these modes seriously limit the high-pressure operation in long-pulse discharges.

Inside the magnetic island the pressure profile is locally flattened, and the pressure gradient is nearly absent. The consequent lack of bootstrap current enhances the NTM instability and makes the island grow. Stabilization of the NTM mode can be achieved by localized deposition of an additional current that compensates for the current lost when an island grows [5], [6]. Electron Cyclotron Current Drive (ECCD) has been proved experimentally in several tokamaks (ASDEX-U [7], [8], [9], DIII-D [10], [11], JT-60U [12]) as an effective method to stabilize NTMs. However, before current drive suppresion can be used effectively in a reactor-grade plasma, several control challenges must be overcome. In particular, neither the absolute position of the island nor the relative position between island and EC beam can be accurately estimated. Only a noisy estimate of the island width is available in real time.

Search & Suppress methods are usually used to align the ECCD with the island. When the estimated island width exceeds a specified threshold, the plasma control system is put into a Search & Suppress mode to make either small rigid radial position shifts of the entire plasma (and thus the island) or small changes in the toroidal field (and thus the ECCD location) to find and lock onto the optimum position for complete island suppression by ECCD. The plasma control system thus executes a "blind search" by changing the relative position between the island and the ECCD deposition location. A typical dwell time of 100 ms allows for checking if the mode amplitude decreases or not. If the mode does decrease, but at a rate slower than a specified threshold rate, a further step and dwell is made. Upon encountering a specified limit in the search parameter without satisfactory mode suppression, the search reverses direction. Once the mode is suppressed, the plasma control system freezes the search parameter until such time as the mode reappears. This approach has been successfully applied to real-time and sustained stabilization of both the $3/2$ and $2/1$ NTM (not simultaneously) in DIII-D [10], [13].

Making use of the island width estimate, a real-time, non-model-based adaptive controller based on extremum seeking [14] is proposed in this paper for beam steering in order to minimize the misalignment between the island

This work was supported by the NSF CAREER award program (ECCS-0645086). W. Wehner and E. Schuster (schuster@lehigh.edu) are with the Department of Mechanical Engineering and Mechanics, Lehigh University, Bethlehem, PA 18015, USA.

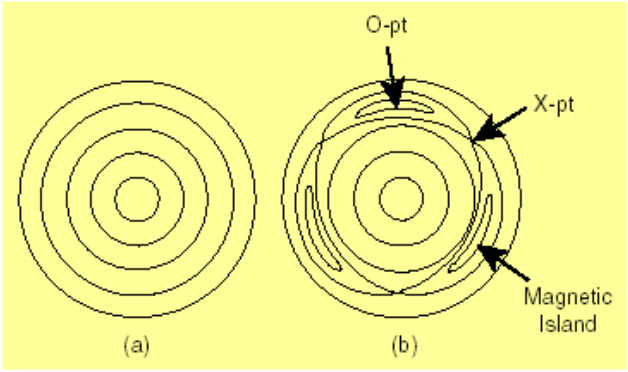

Fig. 1. Magnetic surface topology in (a) ideal MHD plasmas, (b) resistive plasma with magnetic island at the m/n=3/2 flux surface [17].

and the EC beam, and the time (control energy) required for NTM stabilization. The duty cycle and phase of a potential modulation of the EC beam are also considered as control parameters. The modified Rutherford equation [8], widely used to compute the time evolution of an island width, is employed in this work to carry out the simulation studies. The $q = m/n = 3/2$ NTM is considered in this paper, since, it is most often the first mode to significantly reduce confinement [15]. Previous applications of extremum seeking to fusion include [16].

The paper is organized as follows. Section II describes the model used to calculate the effect of ECCD on the island growth rate. Section III defines the NTM control problem and describes the Search & Suppress algorithm. An Extremum Seeking method for NTM stabilization is introduced in Section IV . Simulation results are presented in section V and conclusions are discussed in section VI.

II. Numerical Model

The growth dynamics of tearing mode islands in response to applied ECCD is governed by the modified Rutherford equation [10],

$$\frac{\tau_R}{r}\frac{dw}{dt} = \Delta' r + \epsilon^{1/2}\left[\frac{L_q}{L_p}\right]\beta_p\left[\frac{rw}{w^2+w_d^2} - \frac{rw_{pol}^2}{w^3}\right] - r\Delta_{cd} \quad (1)$$

$$\Delta_{cd} = \epsilon^{1/2}\left[\frac{L_q}{L_p}\right]\beta_p\frac{8q\delta_{ec}}{\pi^2 w^2}\left(\frac{\eta j_{ec}}{j_{bs}}\right) \quad (2)$$

$$\eta = \eta_0\left(1+\frac{2\delta_{ec}^2}{w^2}\right)^{-1} e^{-(5\Delta R/3\delta_{ec})^2} \quad (3)$$

where w is the island width, r is the minor radius at which the NTM is resonant, Δ' is the dimensionless tearing stability index, τ_R is the island resistive diffusion time, β_p is poloidal beta (ratio of plasma pressure to poloidal magnetic field pressure), $\epsilon = r/R_0$ is the local inverse aspect ratio for major radius R_0, w_d is the characteristic island width associated with incomplete pressure flattening in the island, and w_{pol} is the characteristic island width associated with the helical polarization current arising from inertial effects. The scale lengths, L_q and L_p, are defined respectively as $L_q \equiv q/(dq/dr) > 0$ and $L_p \equiv -p/(dp/dr) > 0$, where q denotes the safety factor and p the pressure. The Δ_{cd} term in (1) represents the effect of the ECCD, where j_{ec}/j_{bs} is the ratio of the ECCD current density to the local equilibrium bootstrap current density. The ECCD efficiency η for an unmodulated (continuous) beam of width δ_{ec} is given in (3); it accounts for the effect of the misalignment ΔR between ECCD and island center. More physical insight for these terms can be found in [18].

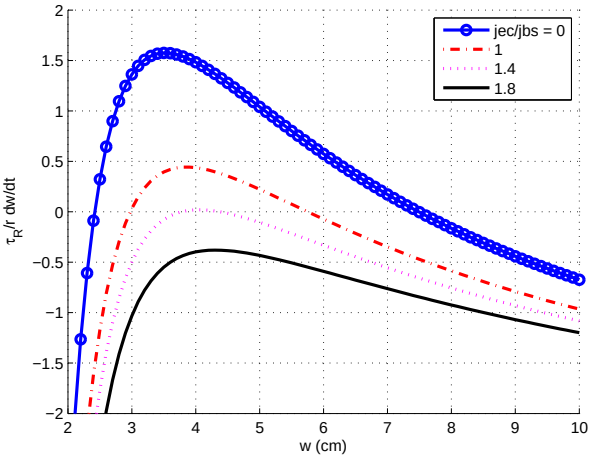

Fig. 2. Normalized growth rate for a 3/2 NTM ($\Delta R = 0$).

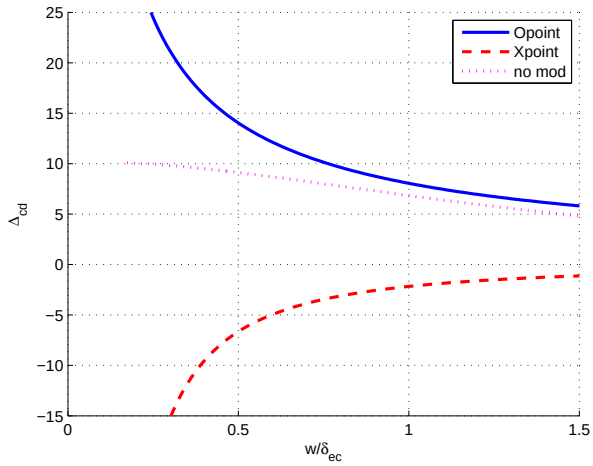

Fig. 3. Effect of ECCD on island growth rate for no modulation (continuous drive), 50/50 duty-cycle O-point modulation, and 50/50 duty-cycle X-point modulation.

Fig. 2 shows the normalized growth rate $\frac{\tau_R}{r}\frac{dw}{dt}$ for different j_{ec}/j_{bs} ratios and perfectly centered ($\Delta R = 0$) current drive. The parameters used for all the numerical studies in this paper are $\beta_p = 0.9$, $\Delta' r = -3$, $r = 36$ cm, $\epsilon^{1/2} = 0.5$, $w_{pol}/r = 0.05$, $w_d/r = 0.028$, $\delta_{ec}/r = 0.08$ and $\eta_0 = 0.4$ [10]. From Fig.2, we can note that j_{ec} must be higher than $1.4 j_{bs}$ for the unmodulated (continuous) ECCD to completely stabilize the NTM. For a smaller j_{ec} the ECCD efficiency must be increased to achieve a full suppression. We adopt $j_{ec}/j_{bs} = 1.8$ in this paper.

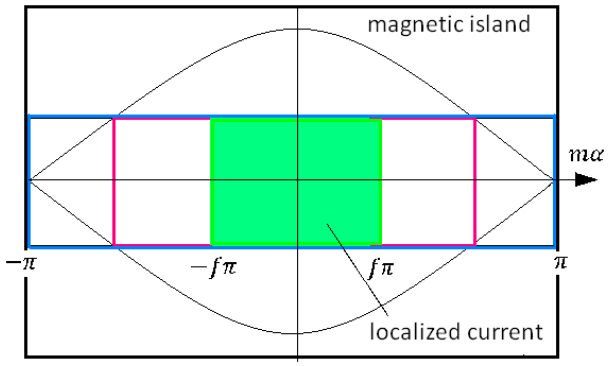

Fig. 4. Localization factor: blue box is area of injected current for CW current drive, green box is area of injected current for modulated current in phase with island O-point.

This efficiency can be increased by modulating the current drive around the O-point (see Fig. 1) and minimizing the amount of current driven outside of the island. Current driven near the island O-point is stabilizing whereas current driven near the island X-point is destabilizing [19]. Fig. 3 shows the effect of a perfectly aligned ($\Delta R = 0$) ECCD on the island growth rate. The Δ_{cd} term is plotted as a function of w/δ_{ec} for both unmodulated (continuous) and modulated current drives. The figure shows the effect of a $50/50$ duty-cycle beam modulated around both the O-point and the X-point. It is possible to note from the figure: i- the destabilizing effect of the modulation around the X-point, ii- the increase of stabilizing effect (i.e., efficiency) of the modulation around the O-point. By denoting the Δ_{cd} term for the perfectly aligned beam ($\Delta R = 0$) as $\hat{\Delta}_{cd}$, we can approximate from Fig. 3 the effect of ECCD modulation as $\hat{\Delta}_{cd}^{(O-point)} = 8.053(w/\delta_e c)^{-0.802}$ and $\hat{\Delta}_{cd}^{(X-point)} = -2.170(w/\delta_e c)^{-1.615}$ [19].

Fig. 4 shows the magnetic island projected on a helical angle coordinate. The ECCD local deposition is illustrated as a function of the localization factor f. The blue box ($f = 1$) represents the current deposition by an unmodulated (or continuous) ECCD. Both the green and pink boxes $f < 1$) represent the current deposition by a modulated current drive centered around the O-point. A localization factor of $f = 0$ would be an ideal instantaneous deposition of current precisely on the island O-point.

To model the change in ECCD effectiveness due to the duty-cycle of the beam modulation, Δ_{cd} is approximated as a linear interpolation between the curves for no modulation and $50/50$ duty-cycle O-point modulation. The effect of the ECCD on the mode growth rate becomes,

$$\Delta_{cd}(\Delta R, \Delta f) = \left[\left(\hat{\Delta}_{cd}^{no-mod} - \hat{\Delta}_{cd}^{O-point}\right)\Delta f + \hat{\Delta}_{cd}^{O-point}\right] e^{-(5\Delta R/3\delta_{ec})^2} \quad (4)$$

where $0 \leq \Delta f \leq 1$ indicates the level of modulation ($\Delta f = 1$: no modulation, $\Delta f = 0$: $50/50$ duty-cycle O-point modulation). In terms of the scheme in Fig. 4, we model the effect of local deposition around the O-point for $0.5 \leq f \leq 1$ (box size).

To model the change in ECCD effectiveness due to the phase of the beam modulation, Δ_{cd} is approximated as a linear interpolation between the curves for $50/50$ duty-cycle X-point modulation and $50/50$ duty-cycle O-point modulation. The effect of the ECCD on the mode growth rate becomes,

$$\Delta_{cd}(\Delta R, \Delta\phi) = \left[\left(\hat{\Delta}_{cd}^{X-point} - \hat{\Delta}_{cd}^{O-point}\right)\Delta\phi + \Delta_{cd}^{O-point}\right] e^{-(5\Delta R/3\delta_{ec})^2} \quad (5)$$

where $0 \leq \Delta\phi \leq 1$ indicates the phase difference between island and current drive ($\Delta\phi = 1$: X-point modulation, $\Delta\phi = 0$: O-point modulation). In terms of the scheme in Fig. 4, we model the effect of the position of the $50/50$ duty-cycle modulated local deposition $f = 0.5$ (position of box center).

III. Search & Suppress Control of NTMs

In order for tokamaks to operate effectively, the plasma must burn at β's above the stability limit for the $3/2$ NTM. Therefore active stabilization of NTMs will be absolutely necessary in reactor-grade tokamaks. The NTMs can be stabilized by replacing the missing bootstrap current by ECCD. Alignment of the ECCD with the island must be achieved with great accuracy for the NTM suppression to be successful. However, real-time reconstruction of the plasma geometry can only locate the island with an accuracy of $1.5-2.0$ cm [13]. Therefore, the position of the island is not available for NTM control. Neither is a precise estimation of the current deposition location. However, a relative measurement of alignment between island and current drive can be determined by modifying the ECCD deposition and measuring the resulting change in island amplitude. Sweeping the ECCD along the plasma will cause the island to shrink as the deposition location nears the island center and to grow back to its saturated size as the deposition location moves away. The most common and successful sweeping approach to NTM stabilization is the Search & Suppress method [13].

The Search & Suppress algorithm, summarized in Fig. 5, steers the beam in a stepwise search to find the optimum ECCD deposition. Once the control is enabled, the algorithm fixes the beam deposition location for a specified dwell time to assess the effect on the magnetic island. If the width of the island decreases by a pre-specified threshold, the algorithm continues to hold the beam deposition location fixed for an additional dwell time. Otherwise, the beam is steered in a step fashion and then held for another dwell period. If the beam position reaches a specified maximum, the step steering direction is reversed (a possible modification of this algorithm consists in reversing the step steering direction if the width of the island does not decrease by the pre-specified threshold for three consecutive step changes). The search-dwell-search procedure continues until the NTM is suppressed. Note that an accurate absolute estimate of the island width is not necessary since it is indeed the island reduction rate what is used as an indication of the quality of the beam-island alignment.

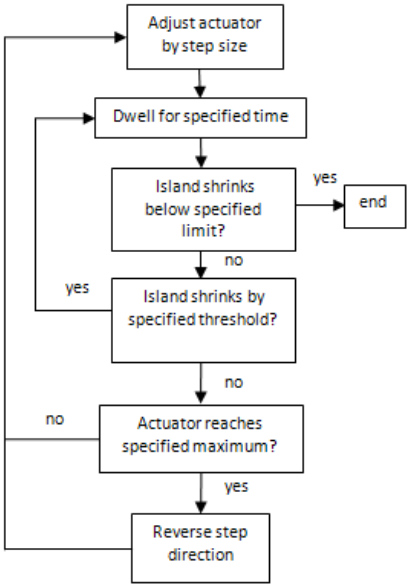

Fig. 5. Standard Search and Suppress Algorithm.

IV. Extremum Seeking Control of NTMs

Extremum seeking control, a popular tool in control applications in the 1940-50's, has seen a resurgence in popularity as a real time optimization tool in different fields of engineering [14]. Extremum seeking is applicable in situations where there is a nonlinearity in the control problem, and the nonlinearity has a local minimum or a maximum. The parameter space can be multidimensional.

The magnetic island width can be considered as the cost functional (J in Fig. 6) and an extremum-seeking adaptive controller can be used to optimally tune those parameters (θ in Fig. 6) affecting the stabilization of the NTM such as ΔR, Δf and $\Delta\phi$ in order to suppress the island. We update the parameters θ after the island width evolves for a pre-specified dwell time which is large enough to reach a converged value, defining in this way a nonlinear static map from the parameters θ to a converged magnetic island width. Thus, we employ the discrete-time variant of extremum seeking [20]. The implementation is depicted in Figure 6, where q denotes here the variable of the Z-transform. The high-pass filter is designed as $0 < h < 1$, and the modulation frequency ω is selected such that $\omega = \alpha\pi$, $0 < |\alpha| < 1$, and α is rational. The static nonlinear block $J(\theta)$ represents the magnetic island width, i.e., $J = w$. If J has a minimum, its value is denoted by J^* and its argument by θ^*. The objective is to minimize J. In our simulation studies we use (1)-(3) to predict the evolution of the island width. Given the island width after the pre-specified dwell time, the output of the nonlinear static map, $J(k) = J(\theta(k))$, after each dwell-time step k, is easily obtained and used to compute $\theta(k+1)$ according to the extremum seeking procedure in Fig. 6, or

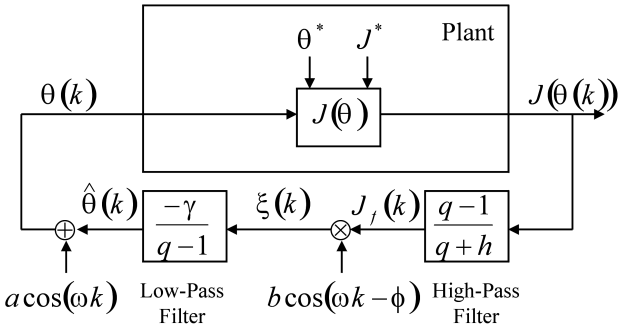

Fig. 6. Extremum seeking control scheme.

written equivalently as

$$J_f(k) = -hJ_f(k-1) + J(k) - J(k-1) \quad (6)$$
$$\xi(k) = J_f(k) b\cos(\omega k - \phi) \quad (7)$$
$$\hat{\theta}(k+1) = \hat{\theta}(k) - \gamma\xi(k) \quad (8)$$
$$\theta(k+1) = \hat{\theta}(k+1) + a\cos(\omega(k+1)), \quad (9)$$

where

$$\theta(k)=\begin{bmatrix}\theta_1(k)\\ \theta_2(k)\\ \vdots\\ \theta_N(k)\end{bmatrix},\ \hat{\theta}(k)=\begin{bmatrix}\hat{\theta}_1(k)\\ \hat{\theta}_2(k)\\ \vdots\\ \hat{\theta}_N(k)\end{bmatrix},\ \xi(k)=\begin{bmatrix}\xi_1(k)\\ \xi_2(k)\\ \vdots\\ \xi_N(k)\end{bmatrix},$$

and N is the number of parameters. The extremum seeking constants shown in Figure 6 are written as

$$a = b = diag([a_1\ \ a_2\ \ \cdots\ \ a_N])$$
$$\gamma = diag([\gamma_1\ \ \gamma_2\ \ \cdots\ \ \gamma_N]).$$

In addition, we denote

$$\cos(\omega k)=\begin{bmatrix}\cos(\omega_1 k)\\ \cos(\omega_2 k)\\ \vdots\\ \cos(\omega_N k)\end{bmatrix},\ \cos(\omega k-\phi)=\begin{bmatrix}\cos(\omega_1 k-\phi_1)\\ \cos(\omega_2 k-\phi_2)\\ \vdots\\ \cos(\omega_N k-\phi_N)\end{bmatrix}.$$

V. Simulation Results

Simulation results for both Search & Suppress and Extremum Seeking algorithms are presented in this section for the parameters given in Section II. In all the simulations we assume that the island has reached saturation before the control scheme is initiated. A 10% proportional noise affects the island width measurement, and a filtered version of the noisy measurement obtained by averaging the last five samples is used for both algorithms (sampling time is $1/40$ of the dwell time).

Fig. 7 shows the performance of the Search & Suppress algorithm detailed in Section III with un-modulated (continuous) current drive. The actuator step size is 0.5 cm, the dwell time is 100 ms, the initial saturated island width is 7.5 cm, and the initial misalignment is $\Delta R_0 = 2.2$ cm. The first few steps marginally decrease the island size, but it is not until the fifth step that the island has decreased sufficiently enough for the algorithm to apply a hold on the actuator. The

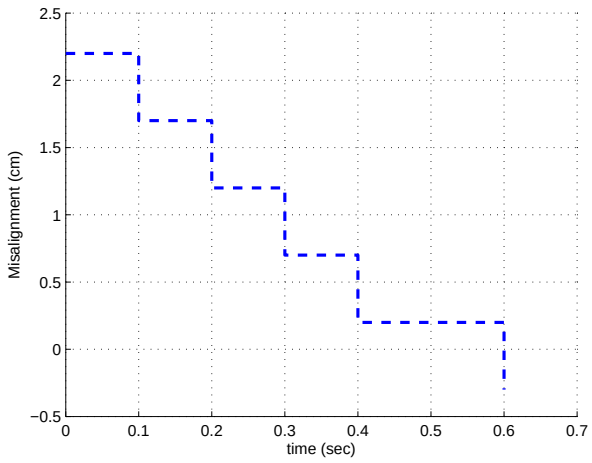

(a)

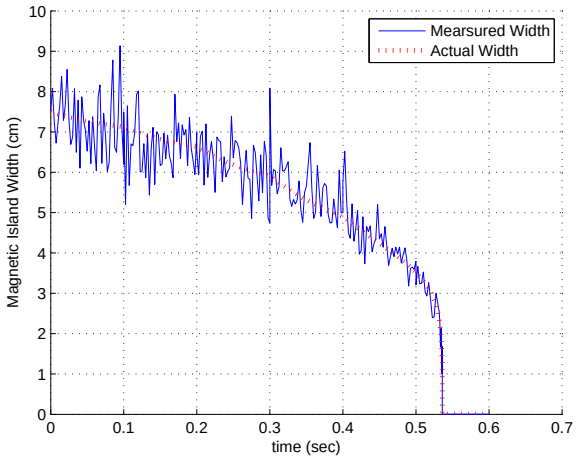

(b)

Fig. 7. Search & Suppress method with un-modulated current drive ($\Delta R_0 = 2.2$ cm): (a) Misalignment (ΔR), (b) Island width: actual width (dashed) and measured width (solid).

suppression time could be reduced by increasing the actuator step size, but that would pose the risk of skipping over the island center. With the model and parameters described in section II the misalignment must be below 0.85 cm to fully suppress the island [10].

The search and suppress algorithm shown in Fig. 7 stabilizes the NTM with an average time of $m = 0.55$ s and standard deviation of $\sigma = 0.14$ s for 100 simulations when the initial misalignment is $\Delta R_0 = 2.2$ cm and there is no modulation of the current drive. With $50/50$ duty-cycle O-point modulation the average suppression time becomes $m = 0.51$ s with standard deviation $\sigma = 0.05$ s. If the initial misalignment is increased to $\Delta R_0 = 2.7$ cm the average suppression time rises to $m = 0.66$ s with standard deviation $\sigma = 0.24$ s for the unmodulated current drive and to $m = 0.6$ s with $\sigma = 0.05$ s for the $50/50$ duty-cycle O-point modulated current drive.

The results above assume that the initial relative position between island and current drive is known, i.e., we know in what direction the beam initially must be moved to converge toward the island. If this information is not available, the initial step direction for the beam must be chosen randomly. In this case the suppression time increases to $m = 1.02$ s with $\sigma = 0.41$ s for no modulation and $m = 0.85$ s with $\sigma = 0.41$ s for $50/50$ duty-cycle O-point modulation when the initial misalignment is $\Delta R_0 = 2.2$ cm, and to $m = 1.03$ s with $\sigma = 0.3$ s for no modulation and $m = 0.85$ s with $\sigma = 0.29$ s for $50/50$ duty-cycle O-point modulation when the initial misalignment is $\Delta R_0 = 2.7$ cm. Additionally, if the initial misalignment is chosen randomly in the range $-2.5 < \Delta R < 2.5$ cm, then the average suppression time is $m = 0.93$ s with $\sigma = 0.46$ s for no modulation and $m = 0.91$ s with $\sigma = 0.41$ s for $50/50$ duty-cycle O-point modulation.

When the modified version of the Search & Suppress algorithm (the step steering direction is reversed if the width of the island does not decrease by the pre-specified threshold for three consecutive step changes) is employed for the random initial step direction case, the suppression time is reduced to $m = 0.80$ s with $\sigma = 0.22$ s for no modulation ($m = 0.67$ s with $\sigma = 0.23$ s for $50/50$ duty-cycle O-point modulation) when the initial misalignment is $\Delta R_0 = 2.2$ cm and to $m = 0.84$ s with $\sigma = 0.22$ s for no modulation ($m = 0.76$ s with $\sigma = 0.26$ s for $50/50$ duty-cycle O-point modulation) when the initial misalignment is $\Delta R_0 = 2.7$ cm. For a random initial misalignment the suppression time is $m = 0.61$ s with $\sigma = 0.23$ s for no modulation and $m = 0.45$ s with $\sigma = 0.26$ for $50/50$ duty-cycle O-point modulation.

Fig. 8 shows the performance of the Extremum Seeking algorithm detailed in Section IV for an un-modulated (continuous) current drive. We consider first the case where only one parameter is optimized: the misalignment $\theta = \Delta R$ (in practice the optimized parameter is the beam deposition location (beam steering)). The extremum seeking parameters have been tuned for optimal suppression time: the modulation and demodulation amplitudes are $a = b = 0.2$ cm, the adaptation gain is $\gamma = -2$ dB, the modulation frequency is $\omega = 0.95\pi$ rad/s, the dwell time is 0.05 s, and the high pass filter parameter h is set to 0.4. For 100 simulations the average suppression time when $\Delta R_0 = 2$ cm is $m = 1.42$ s with standard deviation $\sigma = 0.82$ s for unmodulated current drive and $m = 0.87$ s with standard deviation $\sigma = 0.44$ s for $50/50$ duty-cycle O-point modulated current drive.

The suppression time can be improved by modifying the adaptation gain γ or the probing signal amplitude a as a function of the island width. This gain scheduling approach increases or decreases γ or a as the island grows or shrinks respectively. The type of probing (or dithering) signal can also affect the performance of the extremum seeking method. Typically, sinusoidal waves are employed, as in Fig. 6. But it has been shown that a square wave probing signal can give speedier convergence than the sinusoidal wave probing signal with the same amplitude and frequency. The square wave of unit amplitude and period $2T$ is defined as ($k = 0, 1, \ldots$)

$$sq(t) = \begin{cases} 1 & t \in [2Tk \quad T(2k+1)] \\ -1 & t \in [T(2k+1) \quad 2T(k+1)] \end{cases} \tag{10}$$

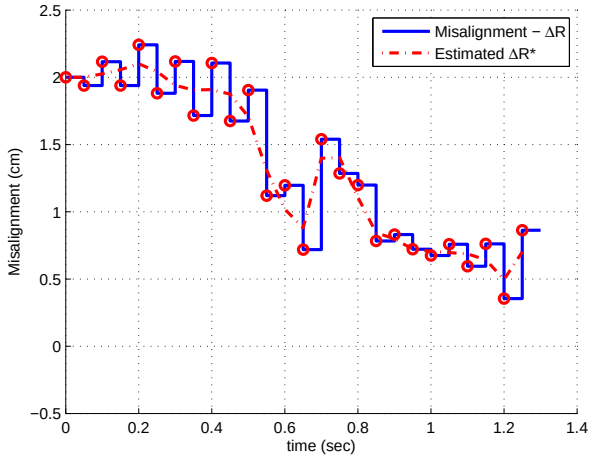

(a)

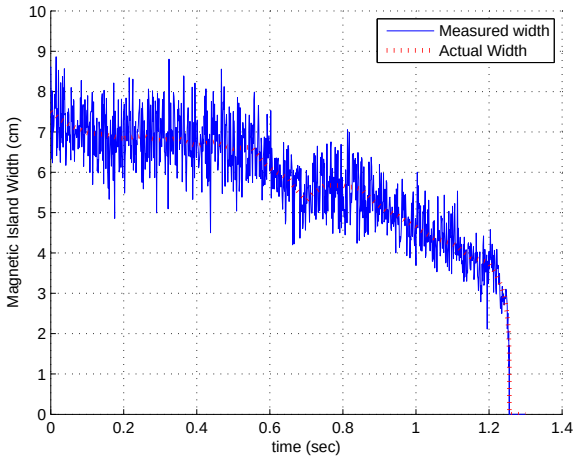

(b)

Fig. 8. Extremum Seeking method with un-modulated current drive ($\Delta R_0 = 2$ cm): (a) Misalignment $\theta = \Delta R$ (solid), estimate $\hat{\theta}$ of optimal misalignment ΔR^* (dashed). The red circles indicate the misalignment being modulated by the probing signal, which is held constant during the dwell time. (b) Island width: actual width (dashed) and measured width with 10% proportional noise (solid).

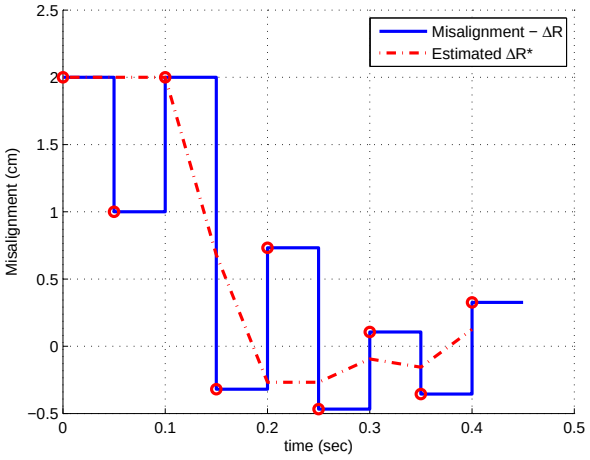

(a)

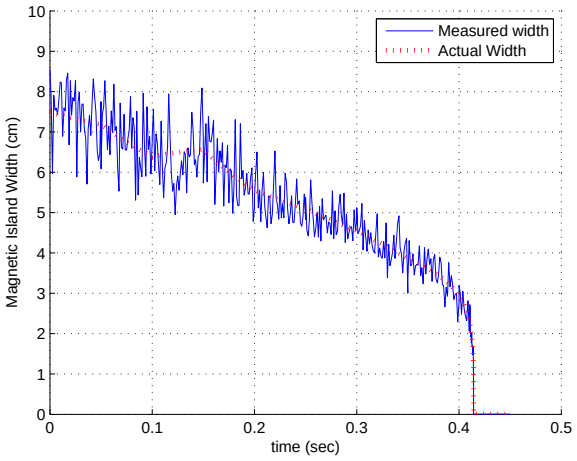

(b)

Fig. 9. Extremum Seeking method with unmodulated current drive, gain scheduling, and square wave dither ($\Delta R_0 = 2$ cm): (a) Misalignment $\theta = \Delta R$ (solid), estimate $\hat{\theta}$ of optimal misalignment ΔR^* (dashed). The red circles indicate the misalignment being modulated by the probing signal, which is held constant during the dwell time. (b) Island width: actual width (dashed) and measured width with 10% proportional noise (solid).

Fig. 9 shows the performance of the Extremum Seeking algorithm with gain scheduling and square-wave dither for an un-modulated (continuous) current drive. The extremum seeking parameters are interpolated from $a = b = 1$ cm, $\gamma = -2db$ to $a = b = 0.2$ cm, $\gamma = -1db$ as a function of the island width. The modulation frequency and dwell time are again $\omega = 0.95\pi$ rad/s and 0.05 s respectively. After 100 simulations the average suppression time when $\Delta R_0 = 2$ cm is $m = 0.48$ s with standard deviation $\sigma = 0.12$ s for unmodulated current drive and $m = 0.31$ s with standard deviation $\sigma = 0.08$ s for $50/50$ duty-cycle O-point modulated current drive. The average suppression time of the Extremum Seeking method is then 4 time steps faster than that of the Search & Suppress algorithm. Even when compared with the case where the Search & Suppress algorithm knows the initial step direction toward the island, the Extremum Seeking method is still 1 time step faster.

We consider now the case where two parameters are optimized by extremum seeking: the misalignment $\theta_1 = \Delta R$ and modulation duty-cycle $\theta_2 = \Delta f$. The extremum seeking parameters for the misalignment are identical to those used in Fig. 8, while the parameters for the modulation duty cycle are $a = b = 0.1$, $\gamma = -1$ db, and $\omega = 0.99\pi$ rad/s. All the simulations assume modulation around the island O-point. Fig. 10 shows the performance of the Extremum Seeking method (sinusoidal probing signal) for a modulated current drive with $\Delta R_0 = 2$ cm and $\Delta f_0 = 1$. As can be noted from Fig. 10(b) the ECCD modulation cannot be adjusted from the continuous drive ($\Delta f = 1$) to the ideal $50/50$ duty-cycle modulation ($\Delta f = 0$) before the island is suppressed, but it is increased enough to reduce the suppression time. The effect of the misalignment on the island shrinkage is comparatively much more significant than the increase of efficiency due to the modulation of the ECCD (compare O-point modulation and no-modulation in Fig. 3). For 100 simulations the average suppression time is $m = 1.31$ s with standard deviation $\sigma = 0.70$ s for $\Delta f_0 = 1$ and $m = 0.98$ s with standard deviation $\sigma = 0.57$ s for $\Delta f_0 = 0.5$ If the

	ES	SS
No mod	0.48 (0.12)	0.80 (0.22)
O-point	0.31 (0.08)	0.67 (0.23)

TABLE I

COMPARISON

Extremum Seeking method is modified with gain scheduling and a square wave dither as described above, the average suppression time is reduced to $m = 0.48$ s with standard deviation $\sigma = 0.1$ s for $\Delta f_0 = 1$ and $m = 0.38$ s with standard deviation $\sigma = 0.07$ s for $\Delta f_0 = 0.5$

It is also of interest to consider the case where the two parameters optimized by extremum seeking are the misalignment $\theta_1 = \Delta R$ and the modulation phase $\theta_2 = \Delta\phi$. Fig. 11 shows the performance of the Extremum Seeking method (sinusoidal probing signal) for a modulated current drive with $\Delta R_0 = 2$ cm and $\Delta\phi_0 = 1/3$. The extremum seeking parameters for the misalignment are the same as those used in Fig. 8, and the parameters for the phase are $a = b = 5/60$, $\gamma = -2db$, and $\omega = 0.99\pi$ rad/s. All the simulations assume a $50/50$ modulation duty cycle. For 100 simulations the average suppression time m and standard deviation σ depend on $\Delta\phi_0$ as follows; $\Delta\phi_0 = 1$ (X-point modulation): $m = 7.62$ s, $\sigma = 4.60$ s, $\Delta\phi_0 = 2/3$: $m = 5.61$ s, $\sigma = 4.60$ s, $\Delta\phi_0 = 1/3$: $m = 2.42$ s, $\sigma = 3.06$ s, $\Delta\phi_0 = 1/6$: $m = 1.81$ s, $\sigma = 1.92$ s, $\Delta\phi_0 = 0$ (O-point modulation): $m = 2.60$ s, $\sigma = 2.54$ s. It is possible to note how the suppression times increase as we approach the $\Delta\phi_0 = 1$ initial condition where the ECCD is modulated around the X-point destabilizing the mode. However, the Extremum Seeking methods succeeds in correcting the modulation phase, driving the modulation to O-point synchronization, and completely suppressing the island.

VI. CONCLUSIONS

Extremum seeking has been proposed as an effective method to stabilize Neoclassical Tearing Modes (NTM) by Electron Cyclotron Current Drive (ECCD) in tokamak plasmas. The effectiveness of extremum seeking in aligning the ECCD with the NTM-driven magnetic island and stabilizing the mode has been compared with a sweeping method. The suppression times for the best versions of the Search & Suppress (the step steering direction is reversed if the width of the island does not decrease by the pre-specified threshold for three consecutive step changes) and Extremum Seeking (gain scheduling and square-wave dither) methods are compared in Table I when the initial relative position between island and current drive is not known. The first number in each entry represents the average suppression time and the second number between parentheses represents the standard deviation for 100 simulations. It has been shown that the Extremum Seeking method has the potential of reducing NTM suppression times.

In addition, it has been shown that the Extremum Seeking method has the ability of modulating simultaneously other parameters beyond island-beam alignment also affecting the effectiveness of the ECCD suppression method such as duty-cycle and phase modulation. Simple models for the dependence of ECCD efficiency on these parameters have been derived from experimental observation.

Future work includes the formulation of more refined models for the efficiency of the ECCD as function of the misalignment, duty-cycle and phase modulation, and also beam power. The elimination of the dwell time and the use of a continuous-time implementation of extremum seeking is also part of our future work.

ACKNOWLEDGEMENTS

We gratefully acknowledge Dr. David A. Humphreys and Dr. Anders Wellander from General Atomics, San Diego, USA, for helpful discussions.

REFERENCES

[1] J. P. Freidberg, *Ideal magnetohydrodynamics*. Plenum Press, New York, 1987.

[2] M. L. Walker, D. A. Humphreys, D. Mazon, D. Moreau, M. Okabayashi, T. H. Osborne, and E. Schuster, "Emerging applications in tokamak plasma control. Control solutions for next-generation tokamaks," *IEEE Control System Magazine*, vol. 26, no. 2, pp. 35–63, April 2006.

[3] R. Buttery *et al.*, "Onset of neoclassical tearing modes on JET," *Nuclear Fusion*, vol. 43, no. 2, pp. 69–83, 2003.

[4] F. Halpern, G. Bateman, and A. Kritz, "Integrated simulations of saturated neoclassical tearing modes in DIII-D, JET, and ITER plasmas," *Physics of Plasmas*, vol. 13, no. 1, 2006.

[5] C. Hegna and J. Callen, "On the stabilization of neoclassical magnetohydrodynamic tearing modes using localized current drive or heating," *Physics of Plasmas*, vol. 4, no. 8, pp. 2940–6, 1997.

[6] H. Zohm, "Stabilization of neoclassical tearing modes by electron cyclotron current drive," *Physics of Plasmas*, vol. 4, no. 9, pp. 3433–5, 1997.

[7] H. Zohm *et al.*, "Experiments on neoclassical tearing mode stabilization by ECCD in ASDEX Upgrade," *Nuclear Fusion*, vol. 39, no. 5, pp. 577–580, 1999.

[8] ——, "The physics of neoclassical tearing modes and their stabilization by ECCD in ASDEX Upgrade," *Nuclear Fusion*, vol. 41, no. 2, pp. 191–202, 2001.

[9] G. Gantenbein *et al.*, "Complete suppression of neoclassical tearing modes with current drive at the electron-cyclotron-resonance frequency in ASDEX upgrade tokamak," *Physical Review Letters*, vol. 85, no. 6, pp. 1242–5, 2000.

[10] R. J. LaHaye *et al.*, "Control of neoclassical tearing modes in DIII-D," *Physics of Plasmas*, vol. 9, no. 5, pp. 2051–60, 2002.

[11] R. Prater *et al.*, "Discharge improvement through control of neoclassical tearing modes by localized ECCD in DIII-D," *Nuclear Fusion*, vol. 43, no. 10, pp. 1128–1134, 2003.

[12] A. Isayama *et al.*, "Complete stabilization of a tearing mode in steady state high-β_p H-mode discharges by the first harmonic electron cyclotron heating/current drive on JT-60U," *Plasma Physics and Controlled Fusion*, vol. 42, no. 12, pp. L37–45, 2000.

[13] D. A. Humphreys, "Active control for stabilization of neoclassical tearing modes," *Physics of Plasmas*, vol. 13, 2006.

[14] K. Ariyur and M. Krstic, *Real-Time Optimization by Extremum Seeking Feedback*. Wiley, 2003.

[15] R. J. LaHaye, "Higher stable beta by use of pre-emptive ECCD in DIII-D," *Nuclear Fusion*, vol. 45, pp. L37–L41, 2005.

[16]

[17] R. J. LaHaye, "Neoclassical tearing modes and their control," *Physics of Plasmas*, vol. 13, p. 055501, 2006.

[18] ——, "Dimensionless scaling of the critical beta for onset of a neoclassical tearing mode," *Physics of Plasmas*, vol. 7, pp. 3349–3359, 2000.

[19] H. Zohm, "Control of MHD instabilities by ECCD: ASDEX upgrade results and implications for ITER," *Nuclear Fusion*, vol. 47, pp. 228–232, 2007.

[20] J.-Y. Choi, M. Krstic, K. Ariyur, and J. Lee, "Extremum seeking control for discrete-time systems," *IEEE Transactions on Automatic Control*, vol. 47, no. 2, pp. 318–323, 2002.

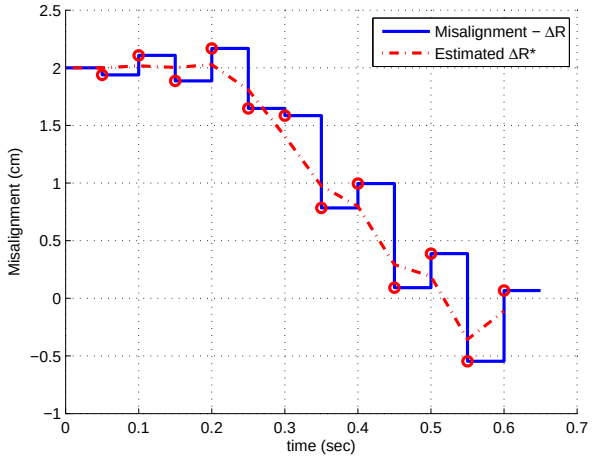

(a)

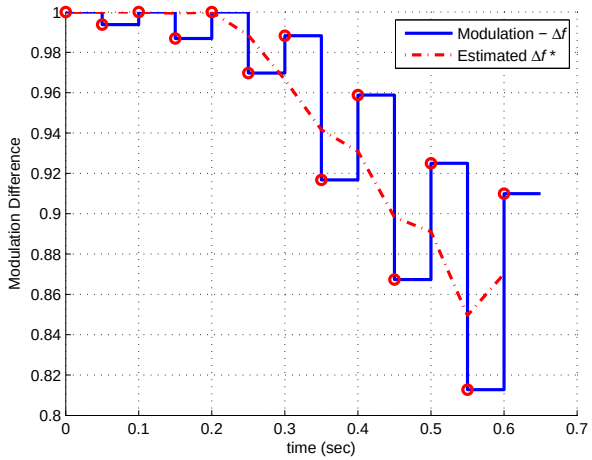

(b)

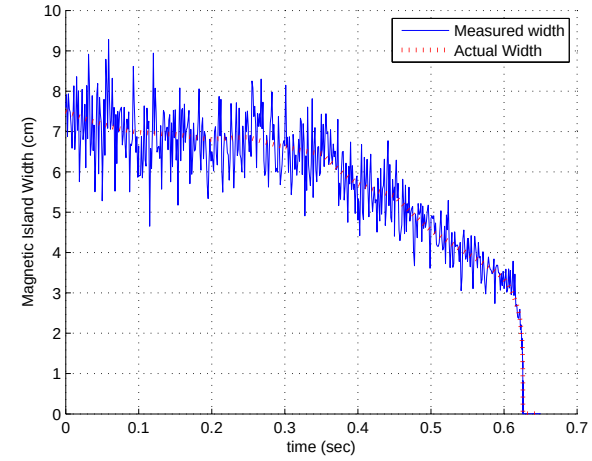

(c)

Fig. 10. Extremum Seeking with modulated current drive ($\Delta R_0 = 2$ cm, $\Delta f_0 = 1$): (a) Misalignment $\theta_1 = \Delta R$ (solid), estimate $\hat{\theta}_1$ of optimal misalignment ΔR^* (dashed). The red circles indicate the misalignment being modulated by the probing signal, which is held constant during the dwell time. (b) Modulation duty cycle $\theta_2 = \Delta f$ (solid), estimate $\hat{\theta}_2$ of optimal duty cycle Δf^* (dashed). The red circles indicate the duty cycle being modulated by the probing signal, which is held constant during the dwell time. (c) Island width: actual width (dashed) and measured width with 10% proportional noise (solid).

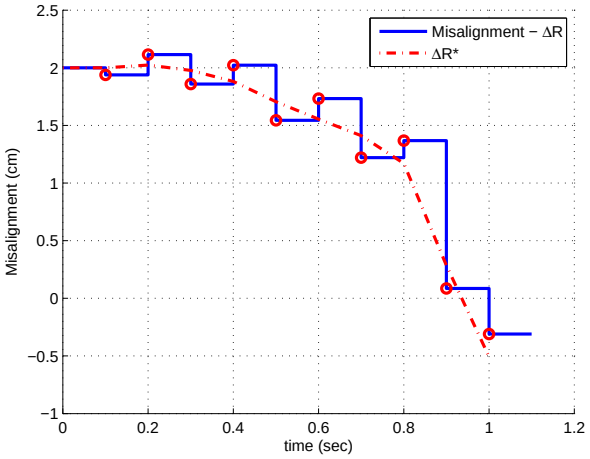

(a)

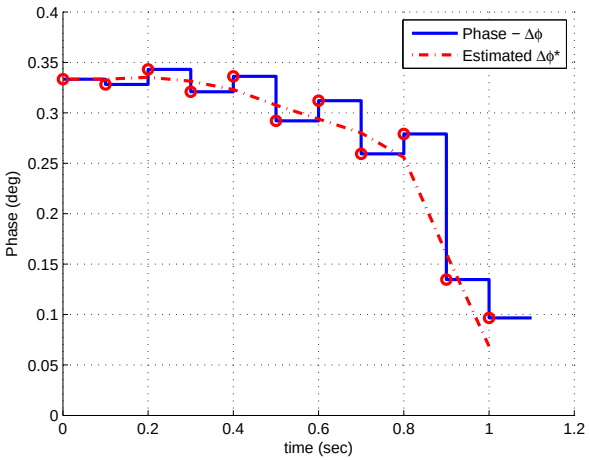

(b)

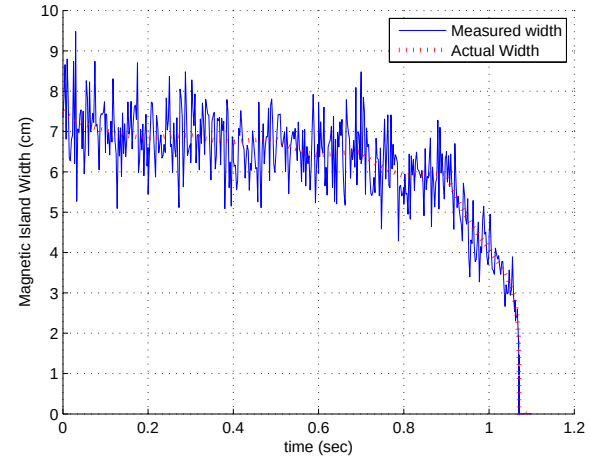

(c)

Fig. 11. Extremum Seeking with modulated current drive ($\Delta R_0 = 2$ cm, $\Delta \phi_0 = 1/3$): (a) Misalignment $\theta_1 = \Delta R$ (solid), estimate $\hat{\theta}_1$ of optimal misalignment ΔR^* (dashed). The red circles indicate the misalignment being modulated by the probing signal, which is held constant during the dwell time. (b) Modulation phase $\theta_2 = \Delta \phi$ (solid), estimate $\hat{\theta}_2$ of optimal phase $\Delta \phi^*$ (dashed). The red circles indicate the duty cycle being modulated by the probing signal, which is held constant during the dwell time. (c) Island width: actual width (dashed) and measured width with 10% proportional noise (solid).